Sains Malaysiana 51(6)(2022): 1733-1751
http://doi.org/10.17576/jsm-2022-5106-11

Study on the Anti-Inflammatory Mechanism of Volatile Components of Hebei *Aster tataricus* Before and After Honey-Fried Based on Gas Chromatography-Mass Spectrometry and Network Pharmacology

(Kajian Mekanisme Anti-Radang Komponen Meruap Hebei *Aster tataricus* Sebelum dan Selepas Digoreng dengan Madu Berdasarkan Kromatografi Gas-Spektrometri Jisim dan Farmakologi Rangkaian)

LIJUAN LV[1], XIANGPEI WANG[2], HONGMEI WU[1,*], KE ZHONG[1] & FENG XU[1]

[1]*Department of Pharmacognosy, Guizhou University of Traditional Chinese Medicine, Guiyang, Guizhou, China*
[2]*National Medical College, Guizhou Minzu University, Guiyang, Guizhou, China*

Received: 27 July 2021/Accepted: 2 November 2021

ABSTRACT

Aster tataricus (AT) and honey-fried *Aster tataricus* (HAT) have a significant effect on relieving cough and reducing sputum, both of which contain many volatile components. Studies have shown that the volatile components of AT and HAT may have an anti-inflammatory effect, but the mechanism is unclear. This study aimed to analyze the daodi herb of Hebei AT and HAT qualitatively and quantitatively using gas chromatography-mass spectrometry and systematically explored the similarities and differences of anti-inflammatory molecular mechanisms of volatile components Hebei AT and HAT by using network pharmacology. These results indicate that there are significant differences in volatile compositions and percentage contents between AT and HAT. Moreover, the anti-inflammatory mechanism of volatile components of Hebei AT and HAT have more prominent similarities and fewer differences. AT and HAT's similar potential active components such as humulene,γ-muurolene, α-phellandrene, and acetic acid were nine. The similar key gene targets were forty-seven, such as CAT, GAPDH, HMOX1, and CTH. The potential active ingredients peculiar to HAT were furfural, β-elemene, methyleugenol, and unique targets of EIF6 and PKIA. It suggests that HAT had its characteristics in clinical anti-inflammatory. Their active anti-inflammatory components and percentage contents were different, and HAT was higher than that of AT. The anti-inflammatory effect of volatile components of HAT may be better than that of AT. These results provide a theoretical basis for the study of the anti-inflammatory molecular mechanism of AT and HAT.

Keywords: Anti-inflammatory; *Aster tataricus*; honey-fried; volatile components

ABSTRAK

Aster tataricus (AT) dan *Aster tataricus* (HAT) goreng madu mempunyai kesan yang ketara bagi melegakan batuk dan mengurangkan kahak, kedua-duanya mengandungi banyak komponen yang meruap. Kajian telah menunjukkan bahawa komponen meruap AT dan HAT mungkin mempunyai kesan anti-radang, tetapi mekanismenya tidak jelas. Kajian ini bertujuan untuk menganalisis herba daodi Hebei AT dan HAT secara kualitatif dan kuantitatif menggunakan kromatografi gas-spektrometri jisim dan secara sistematik bagi meneroka persamaan dan perbezaan mekanisme molekul anti-radang komponen meruap Hebei AT dan HAT dengan menggunakan farmakologi rangkaian. Keputusan menunjukkan bahawa terdapat perbezaan yang signifikan dalam komposisi komponen meruap dan kandungan peratusan antara AT dan HAT. Selain itu, mekanisme anti-radang komponen yang meruap pada Hebei AT dan HAT mempunyai lebih banyak persamaan dan hanya sedikit perbezaan. Komponen sama aktif berpotensi AT dan HAT seperti humulena, γ-muurolene, α-phellandrene dan asid asetik adalah sembilan. Sasaran gen utama yang sama ialah empat puluh tujuh, seperti CAT, GAPDH, HMOX1 dan CTH. Bahan aktif yang berpotensi khusus untuk HAT ialah furfural, β-elemene, metileugenol dan sasaran unik EIF6 dan PKIA. Ia menunjukkan bahawa HAT mempunyai ciri-cirinya dalam anti-radang klinikal. Komponen anti-radang aktif dan kandungan peratusannya berbeza dan HAT lebih tinggi daripada AT. Kesan anti-radang komponen meruap pada HAT lebih baik daripada AT. Keputusan ini memberikan asas teori untuk kajian mekanisme molekul anti-radang AT dan HAT.

Kata kunci: Anti-radang; *Aster tataricus*; goreng madu; komponen yang meruap

Introduction

Aster tataricus (AT) is derived from the dry roots and rhizomes of Compositae plant *Aster tataricus* L.f., which is first recorded in 'Shen Nong Ben Cao Jing', has a long history of clinical application in China (Su & Liu 2011). It has the effect of moistening the lung to lower qi, relieving cough and reducing sputum (National Pharmacopoeia Commission 2020). AT is mainly produced in Hebei, Anhui, Henan, Gansu, North and Northeast China. Among them, the annual output of Hebei AT was more than 60% of the whole country, with high yield and good quality. AT plays an important role in medicine for relieving cough and reducing sputum; it is often used in raw thick slices and honey-fried processing (Fang et al. 2012). The processing method of honey-fried *Aster tataricus* (HAT) is to take cooked honey, add an appropriate amount of boiling water to dilute it, add it into AT slices, mix well, moisten it until it is transparent, put it in a frying container, heat it with soft fire, fry it until it is brown, and take it out to cool when it is not sticky (Gong 2016). The method of processing traditional Chinese medicine (TCM) is the characteristics and advantages of TCM, and it is the first batch of intangible cultural heritage in China (Li et al. 2020).

It has been reported that HAT has a better effect than AT in eliminating phlegm, which indicated that the processing method affected AT's eliminating phlegm effect (Wu et al. 2006). Pharmacodynamic experiments showed that relieving cough and reducing sputum is closely related to inflammation (Li et al. 2021), volatile components of TCM have an anti-inflammatory effect (Zhang & Li 2017), and AT has an anti-inflammatory effect after compatibility of TCM (Li et al. 2009). It is suggested that the volatile components of AT and HAT may have an anti-inflammatory effect. Inflammation is a common clinical symptom associated with the occurrence and development of various diseases (Dutta et al. 2019). Therefore, how to reduce the occurrence of inflammation effectively has become a hot topic in clinical research.

Network pharmacology is a new technology that integrates many subjects. It is consistent with the holistic and systematic research concept of TCM and the characteristics of multi-component and multi-level coordination. It can comprehensively explore the correlation between active components and active targets and diseases (Guo et al. 2021). The combination of network pharmacology and gas chromatography-mass spectrometry (GC-MS) are helpful to clarify the potential complex relationship between multi-component and multi-target when the volatile components of the dao-di herb Hebei AT before and after honey-fried play an anti-inflammatory role. Finally, the screening results of network pharmacology were verified by molecular docking. The research results will provide a basis for clinical rational drug use of AT.

Materials and Methods

Experimental materials and instruments

Samples of Hebei AT and HAT were purchased from the medicinal materials market and identified as AT and HAT derived from the dry roots and rhizomes of Compositae plant *Aster tataricus* L.f. by professor Xiangpei Wang of Guizhou Minzu University. GC-MS analysis was carried out using an HP6890/5975C GC-MS spectrometer (Agilent USA) equipped with an HP-5MS (60 m×0.25 mm×0.25 μm) stone elastic capillary column.

The solid-phase microextraction procedure

The accurately weighed AT and HAT (1.000g) were placed into 25 mL of solid-phase microextraction sampling bottles, respectively, and then, inserted into a manual injector with a 2 cm-50/30 um DVB/CAR/PDMS Stableflex fibre head. The temperature of the headspace vial was kept at 60 ℃, exposed to the sample headspace for 60 min. The extraction head was removed from sample vials and immediately inserted onto the gas chromatography injection port (temperature of 250 ℃), the sample thermal desorption and then directly injected into gas chromatography.

GC-MS analysis

The analysis of gas chromatography used an HP-5MS (60 m × 0.25 mm × 0.25 μm) stone elastic capillary column. High purity helium (purity 99.99 %) and the pre-column pressure was 15.85 psi, which were used as carrier gas with a flow rate of 1.0 $mLmin^{-1}$, samples were injected in splitless mode. The gas chromatography initial temperature was programmed to hold at 40 ℃ for 2 min, temperature increased to 180 ℃ at 3.5 $℃min^{-1}$, then to increase to 260 ℃ at 10 $℃min^{-1}$, running 50 min. The injector temperature was set at 250 ℃. The solvent delay was 3 min. The mass spectrometer was operated in the electron impact (EI) mode by using ionization energy at 70 eV with an ionization source temperature

of 230 ℃ and a quadrupole temperature set of 150 ℃. The emission current was 34.6 uA, the multiplier voltage was 1847 V, the interface temperature was 280 ℃, and the mass range was 29-500 amu.

DATA ANALYSIS

The mass spectrometer computer data system retrieved each peak in the total ion flow map. The volatile chemical components were determined by the standard mass spectra of NIST17 and Wiley 275. Then the relative concentration of each chemical composition was determined by the peak area normalization method.

MOLECULAR STRUCTURE AND TARGET PROTEIN PREDICTION

The molecular structures of the volatile compounds were obtained from the PubChem database (https://pubchem.ncbi.nlm.nih.gov/), and the 3D structures were downloaded in .sdf format. The action chemical constituents were screened by the TCMSP database with ADME parameters (oral bioavailability≥30% and drug-likeness≥0.18), and the related anti-inflammatory active ingredients reported in the literature were used as the standard (Feng et al. 2015; Fink et al. 2015; Labib et al. 2017; Li et al. 2015; Lin 2011; Lin et al. 2020; Ninomiya et al. 2013; Queiroz et al. 2014; Saeed et al. 2012; Sakhaee et al. 2020; Sousa et al. 2020; Yang et al. 2019). Inflammation related target proteins were retrieved from a comprehensive database of human genes and gene phenotypes (OMIM, http://www.omim.org/) and GeneCards database (https://www.genecards.org/). Finally, the screened targets were converted into UniProt ID format with the UniProt database (https://www.uniprot.org/).

NETWORK CONSTRUCTION AND TOPOLOGIC PROFILE ANALYSIS

AT and HAT's active components, targets, and inflammatory targets were connected to form a 'component-target-disease' network. The above network was visually analyzed using Cytoscape 3.7.2 software, the degree, betweenness centrality and closeness centrality of each node were obtained. Proteins showing values greater than the median value for the above three topological parameters at all nodes were regarded as the anti-inflammatory response's key target (Huang et al. 2020).

GO AND KEGG ENRICHMENT ANALYSIS

Protein interaction analysis of the selected targets was carried out by using the STRING database (http://string-db.org). Then, the database DAVID (https://david.ncifcrf.gov/) was carried out to analyze the KEGG pathway and the biological process of GO (Gene Ontology).

MOLECULAR DOCKING

Molecular docking was carried out using the DockThor (Santos et al. 2020), which applied a rigid protein and a flexible ligand to docking and illustrates how a ligand acts on a complex molecular network. Finally, it was visualized in Ligplot.

Results and Discussion

IDENTIFICATION AND ANALYSIS OF VOLATILE COMPONENTS

A total of sixty-three volatile components were identified in AT sample by GC-MS analysis (Figure 1), the main components were 1-pentadecene (7.226%), β-pipene (3.091%), longicyclene (1.618%), acetic acid (1.591%), and α-terpinolene (1.418%). A total of fifty-nine volatile components were identified in the HAT sample by GC-MS analysis (Figure 2), the main components were 1-pentadecene (2.310%), acetic acid (2.060%), β-pipene (1.805%), furfural (1.661%), and bicyclogermacrene (1.631%). The main volatile components were alkenes, aldehydes, alcohols, and esters. There were forty-seven similar volatile components in AT and HAT, and the main components were 1-pentadecene, β-pipene, and acetic acid. AT had sixteen unique volatile components, the main components were ledene; p-(1-propenyl)-toluene; 1, 8, 11, 14-heptadecatetraene; cedrol. HAT had 12 unique volatile components, and the main component was furfural, bicyclogermacrene, 5-methyl-2-furancarboxaldehyde. The results showed that there were significant differences in volatile compositions and percentage contents between AT and HAT. The chemical constituents of AT changed during honey-fried. After processing, HAT reduced sixteen volatile components and increased twelve volatile components. The corresponding volatile components are listed in Figure 3 and Tables 1 and 2.

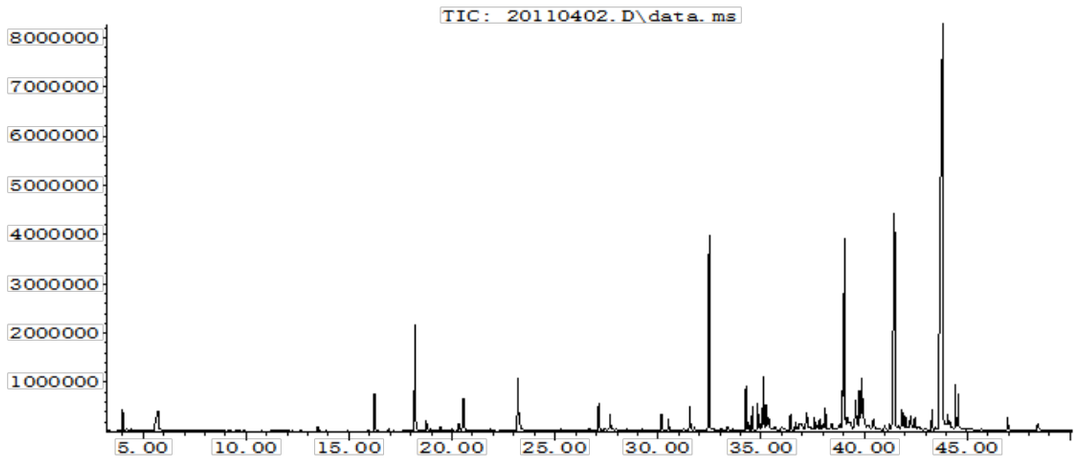

FIGURE 1. TIC of volatile components extracted from AT

TABLE 1. Percentages of volatile components extracted from AT

No.	Retention time (min)	Compound name	Formula	Molecular weight	The percentage (%)
1	4.437	Ethanol	C_2H_6O	46	0.033
2	5.726	Acetic acid	$C_2H_4O_2$	60	1.591
3	6.484	3-Methylbutanal	$C_5H_{10}O$	86	0.006
4	6.673	2-Methylbutanal	$C_5H_{10}O$	86	0.005
5	15.917	α-Thujene	$C_{10}H_{16}$	136	0.020
6	16.23	α-Pinene	$C_{10}H_{16}$	136	1.016
7	16.843	α-Fenchene	$C_{10}H_{16}$	136	0.010
8	16.923	Camphene	$C_{10}H_{16}$	136	0.074
9	17.713	Benzaldehyde	C_7H_6O	106	0.128
10	18.033	sabinene	$C_{10}H_{16}$	136	0.018
11	18.196	β-pipene	$C_{10}H_{16}$	136	3.091
12	18.747	β-Myrcene	$C_{10}H_{16}$	136	0.394
13	19.422	α-Phellandrene	$C_{10}H_{16}$	136	0.169
14	19.977	α-terpipene	$C_{10}H_{16}$	136	0.099
15	20.333	p-Cymene	$C_{10}H_{14}$	134	0.276
16	20.533	Limonene	$C_{10}H_{16}$	136	0.655
17	20.554	β-Phellandrene	$C_{10}H_{16}$	136	0.935
18	21.868	γ-Terpinene	$C_{10}H_{16}$	136	0.128
19	22.425	1-(1H-pyrrol-2-yl)-Ethanone	C_6H_7NO	109	0.053
20	22.506	Acetophenone	C_8H_8O	120	0.085
21	23.189	α-terpinolene	$C_{10}H_{16}$	136	1.418
22	23.230	p-(1-Propenyl)-toluene	$C_{10}H_{12}$	132	0.839

23	23.649	Linalool	$C_{10}H_{18}O$	154	0.065
24	24.264	1,3,8-p-Menthatriene	$C_{10}H_{14}$	134	0.030
25	24.363	Fenchol	$C_{10}H_{18}O$	154	0.057
26	26.541	Pinocarvone	$C_{10}H_{14}O$	150	0.015
27	26.657	endo-Borneol	$C_{10}H_{18}O$	154	0.131
28	27.117	Terpinen-4-ol	$C_{10}H_{18}O$	154	0.987
29	27.419	p-Cymen-8-ol	$C_{10}H_{14}O$	150	0.140
30	27.665	α-Terpineol	$C_{10}H_{18}O$	154	0.610
31	27.818	Dodecane	$C_{12}H_{26}$	170	0.081
32	29.825	Benzaldehyde, 4-(1-methylethyl)-	$C_{10}H_{12}O$	148	0.015
33	30.164	Bicyclo[2.2.1]heptane-2-carboxylic acid, 3,3-dimethyl-, methyl ester	$C_{11}H_{18}O_2$	182	0.554
34	31.541	Bornyl acetate	$C_{12}H_{20}O_2$	196	0.767
35	33.072	Myrtenyl acetate	$C_{12}H_{18}O_2$	194	0.082
36	34.076	α-Cubebene	$C_{15}H_{24}$	204	0.027
37	34.257	α-Longipinene	$C_{15}H_{24}$	204	1.335
38	34.377	Neryl acetate	$C_{12}H_{20}O_2$	196	0.363
39	34.989	Ylangene	$C_{15}H_{24}$	204	0.183
40	35.098	longicyclene	$C_{15}H_{24}$	204	1.618
41	35.22	(-)-trans-Myrtanyl acatate	$C_{12}H_{20}O_2$	196	0.690
42	35.687	Tetradecane	$C_{14}H_{30}$	198	0.181
43	36.164	β-Longipinene	$C_{15}H_{24}$	204	0.060
44	36.428	Longifolene	$C_{15}H_{24}$	204	0.519
45	37.212	γ-Elemene	$C_{15}H_{24}$	204	0.863
46	37.584	Aromandendrene	$C_{15}H_{24}$	204	0.407
47	37.837	cis-β-Farnesene	$C_{15}H_{24}$	204	0.334
48	37.993	α-Himachalene	$C_{15}H_{24}$	204	0.232
49	38.109	Humulene	$C_{15}H_{24}$	204	0.691
50	38.823	γ-Muurolene	$C_{15}H_{24}$	204	0.139
51	39.045	1-Pentadecene	$C_{15}H_{30}$	210	7.226
52	39.58	Ledene	$C_{15}H_{24}$	204	1.170
53	39.628	α-Muurolene	$C_{15}H_{24}$	204	0.337
54	39.763	(3S,3aS,8aR)-6,8a-Dimethyl-3-(prop-1-en-2-yl)-1,2,3,3a,4,5,8,8a-octahydroazulene	$C_{15}H_{24}$	204	1.272
55	40.447	δ-Cadinene	$C_{15}H_{24}$	204	0.252
56	41.218	α-Calacorene	$C_{15}H_{20}$	200	0.188
57	41.327	Germacrene B	$C_{15}H_{24}$	204	0.078
58	42.458	Spathulenol	$C_{15}H_{24}O$	220	0.425
59	42.657	(-)-Spathulenol	$C_{15}H_{24}O$	220	0.118
60	43.29	Cedrol	$C_{15}H_{26}O$	222	0.593
61	44.148	Isospathulenol	$C_{15}H_{24}O$	220	0.277
62	44.564	1,8,11,14-Heptadecatetraene, (Z,Z,Z)-	$C_{17}H_{28}$	232	0.812
63	49.171	Hexadecanoic acid, methyl ester	$C_{17}H_{34}O_2$	270	0.039

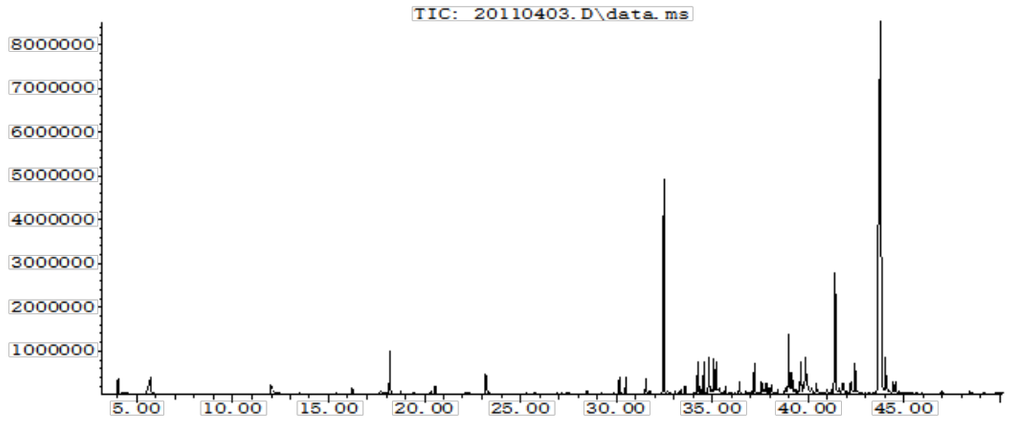

FIGURE 2. TIC of volatile components extracted from HAT

TABLE 2. Percentages of volatile components extracted from HAT

No.	Retention time (min)	Compound name	Formula	Molecular weight	The percentage (%)
1	4.423	Ethanol	C_2H_6O	46	0.093
2	5.715	Acetic acid	$C_2H_4O_2$	60	2.060
3	6.467	3-Methylbutanal	$C_5H_{10}O$	86	0.010
4	6.66	2-Methylbutanal	$C_5H_{10}O$	86	0.013
5	11.764	Pyrazine, methyl-	$C_5H_6N_2$	94	0.025
6	11.967	Furfural	$C_5H_4O_2$	96	1.661
7	13.145	2-Furanmethanol	$C_5H_6O_2$	98	0.107
8	15.424	Ethanone, 1-(2-furanyl)-	$C_6H_6O_2$	110	0.273
9	15.909	α-Thujene	$C_{10}H_{16}$	136	0.066
10	16.229	α-Pinene	$C_{10}H_{16}$	136	0.280
11	16.921	Camphene	$C_{10}H_{16}$	136	0.025
12	17.609	Benzaldehyde	C_7H_6O	106	0.085
13	17.685	5-methyl-2-Furancarboxaldehyde	$C_6H_6O_2$	110	0.534
14	18.02	sabinene	$C_{10}H_{16}$	136	0.207
15	18.187	β-pipene	$C_{10}H_{16}$	136	1.805
16	18.749	β-Myrcene	$C_{10}H_{16}$	136	0.246
17	19.421	α-Phellandrene	$C_{10}H_{16}$	136	0.131
18	19.98	α-terpipene	$C_{10}H_{16}$	136	0.028
19	20.336	p-Cymene	$C_{10}H_{14}$	134	0.140
20	20.553	Limonene	$C_{10}H_{16}$	136	0.612
21	21.867	γ-Terpinene	$C_{10}H_{16}$	136	0.037
22	22.145	Ethanone, 1-(1H-pyrrol-2-yl)-	C_6H_7NO	109	0.330

23	22.4	Acetophenone	C_8H_8O	120	0.185
24	23.189	α-terpinolene	$C_{10}H_{16}$	136	1.283
25	24.261	1,3,8-p-Menthatriene	$C_{10}H_{14}$	134	0.035
26	25.745	4H-Pyran-4-one, 2,3-dihydro-3,5-dihydroxy-6-methyl-	$C_6H_8O_4$	144	0.091
27	27.128	Terpinen-4-ol	$C_{10}H_{18}O$	154	0.098
28	27.426	p-Cymen-8-ol	$C_{10}H_{14}O$	150	0.159
29	27.671	α-Terpineol	$C_{10}H_{18}O$	154	0.058
30	27.811	Dodecane	$C_{12}H_{26}$	170	0.046
31	29.742	Pulegone	$C_{10}H_{16}O$	152	0.036
32	30.164	Bicyclo[2.2.1]heptane-2-carboxylic acid, 3,3-dimethyl-, methyl ester	$C_{11}H_{18}O_2$	182	0.714
33	31.541	Bornyl acetate	$C_{12}H_{20}O_2$	196	0.667
34	33.073	Myrtenyl acetate	$C_{12}H_{18}O_2$	194	0.095
35	34.075	α-Cubebene	$C_{15}H_{24}$	204	0.096
36	34.255	α-Longipinene	$C_{15}H_{24}$	204	1.288
37	34.375	Neryl acetate	$C_{12}H_{20}O_2$	196	0.353
38	34.994	Ylangene	$C_{15}H_{24}$	204	0.132
39	35.099	longicyclene	$C_{15}H_{24}$	204	1.485
40	35.22	(-)-trans-Myrtanyl acatate	$C_{12}H_{20}O_2$	196	1.167
41	35.701	β-elemene	$C_{15}H_{24}$	204	0.402
42	35.984	Methyleugenol	$C_{11}H_{14}O_2$	178	0.142
43	36.164	β-Longipinene	$C_{15}H_{24}$	204	0.064
44	36.429	Longifolene	$C_{15}H_{24}$	204	0.513
45	37.213	γ-Elemene	$C_{15}H_{24}$	204	1.502
46	37.584	Aromandendrene	$C_{15}H_{24}$	204	0.544
47	37.835	cis-β-Farnesene	$C_{15}H_{24}$	204	0.410
48	37.995	α-Himachalene	$C_{15}H_{24}$	204	0.257
49	38.111	Humulene	$C_{15}H_{24}$	204	0.350
50	38.826	γ-Muurolene	$C_{15}H_{24}$	204	0.208
51	39.005	1-Pentadecene	$C_{15}H_{30}$	210	2.310
52	39.627	Bicyclogermacrene	$C_{15}H_{24}$	204	1.631
53	39.758	(3S,3aS,8aR)-6,8a-Dimethyl-3-(prop-1-en-2-yl)-1,2,3,3a,4,5,8,8a-octahydroazulene	$C_{15}H_{24}$	204	0.421
54	40.44	δ-Cadinene	$C_{15}H_{24}$	204	0.506
55	41.215	α-Calacorene	$C_{15}H_{20}$	200	0.169
56	41.628	Nerolidol	$C_{15}H_{26}O$	222	0.156
57	41.781	Germacrene B	$C_{15}H_{24}$	204	0.159
58	42.456	Spathulenol	$C_{15}H_{24}O$	220	1.270
59	49.171	Hexadecanoic acid, methyl ester	$C_{17}H_{34}O_2$	270	0.048

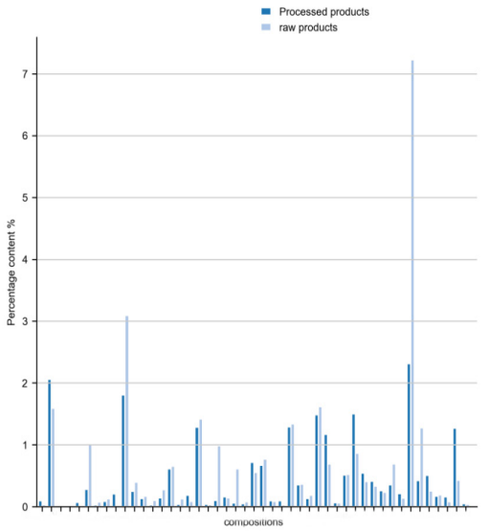

FIGURE 3. Comparison of volatile components in AT before and after honey-fried

MOLECULAR STRUCTURE AND TARGET PROTEIN PREDICTION

This study screened thirty-two volatile anti-inflammatory components of AT and twenty-six volatile anti-inflammatory components of HAT. A total of ten thousand four hundred and thirty genes related to inflammation and protein targets were screened by OMIM and GeneCards database. The targets of AT, HAT and inflammation, were drawn in the Venn diagram (Figure 4). There were nine active anti-inflammatory components in AT and twelve active anti-inflammatory components in HAT, of which there were forty-seven intersection targets of inflammation and AT, forty-nine intersection targets of inflammation and HAT. They represent the potential anti-inflammatory targets of AT and HAT, respectively. The anti-inflammatory targets peculiar to HAT were twenty-six. There were forty-seven similar intersection targets of inflammation in AT and HAT. Which showed similarities and differences in the anti-inflammatory effect of volatile components of AT and HAT.

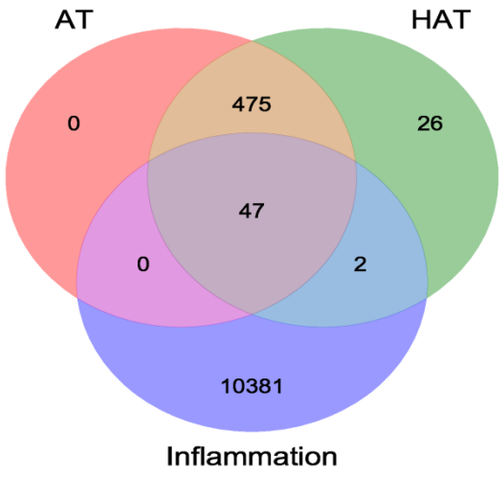

FIGURE 4. Target Venny diagram of inflammation, AT and HAT

NETWORK CONSTRUCTION AND SCREENING OF KEY TARGET PROTEINS

The interaction network of the anti-inflammatory effect of AT and HAT were constructed through Cytoscape 3.7.2 software. The network was visualized with different colours and shapes. The results can be directly shown the network relationship between active ingredients and disease targets. AT and HAT's similar potential active components were nine, including ethanol, acetic acid, benzaldehyde, α-phellandrene, p-cymene, acetophenone, humulene, γ-muurolene and methyl palmitate. The similar potential key targets were forty-seven, including CTSB, CTSD, GPI, HDC, PNP, CBS, F7, KYNU, TNF, AHCY, CAT, CES2, PFKFB4, LYZ, GYS1, GAPDH, ABAT, HMOX1, FDXR, SHMT2, SHMT1, F13A1, UROD, APRT, GSTM1, ANXA3, CPA1, LCMT2, CTH, GNMT, HAGH, GPHN, GSTM4, HDAC8, GAMT, ALOX5, MMUT, PPOX, MPST, ASL, PYCR2, SPR, GGT5, MPO, REN, TREH, and NCOA2. The potential active ingredients peculiar to HAT were furfural, β-elemene, methyleugenol, and unique targets of EIF6, PKIA. It illustrating the anti-inflammatory mechanism of volatile components of Hebei AT before and after honey-fried had more prominent similarities and smaller differences. The results are shown in Figure 5.

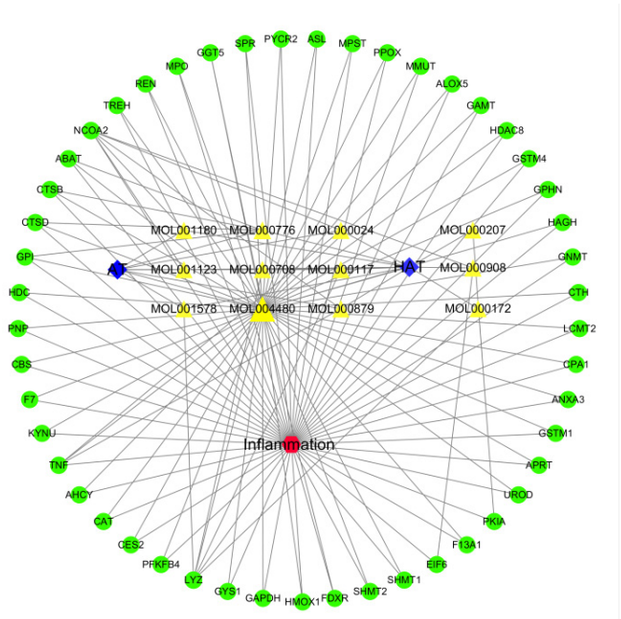

FIGURE 5. 'Component-target-disease' interactive network of the anti-inflammatory of AT and HAT (The yellow triangle represents the active components of anti-inflammatory drugs. The green circle represents the direct targets of anti-inflammatory drugs. The blue diamond represents medicine, and the red hexagon represents inflammation)

AT's three topological parameters (degree, betweenness centrality and closeness centrality) were calculated as 3, 0.00004509 and 0.46825397. The parameters of HAT were calculated as 3, 0.00005237 and 0.46616541. The similar essential gene targets of AT and HAT were 47, including CTSB, CTSD, GPI, HDC, PNP, CBS, F7, KYNU, TNF, AHCY, CAT, CES2, PFKFB4, LYZ, GYS1, GAPDH, ABAT, HMOX1, FDXR, SHMT2, SHMT1, F13A1, UROD, APRT, GSTM1, ANXA3, CPA1, LCMT2, CTH, GNMT, HAGH, GPHN, GSTM4, HDAC8, GAMT, ALOX5, MMUT, PPOX, MPST, ASL, PYCR2, SPR, GGT5, MPO, REN, TREH, and NCOA2, which were all more significant than the median mean. These targets were considered as key targets of the anti-inflammatory effects of the volatile component. Our results predicted that the key anti-inflammatory targets of AT and HAT were the same. The top ten key targets of AT and HAT are shown in Table 3.

TABLE 3. Topological parameter analysis of direct-acting targets in the network

Names	Gene names	Name of the target protein	Betweennesscentrality	Closeness centrality	Degree
AT	LYZ	Lysozyme	0.08914553	0.5	10
AT	NCOA2	Nuclear receptor coactivator 2	0.07629411	0.5	10
AT	TNF	Tumor necrosis factor	0.02738993	0.48360656	7
AT	ABAT	4-aminobutyrate aminotransferase	0.00596034	0.47580645	7
AT	GPI	Glucose-6-phosphate isomerase	0.00596034	0.47580645	5
AT	CTSD	Cathepsin D	0.00596034	0.47580645	5
AT	CTSB	Cathepsin B	0.00596034	0.47580645	5
AT	UROD	Uroporphyrinogen decarboxylase	4.51E-05	0.46825397	3
AT	TREH	Trehalase	4.51E-05	0.46825397	3
AT	SPR	Sepiapterin reductase	4.51E-05	0.46825397	3
HAT	NCOA2	Nuclear receptor coactivator 2	0.04944516	0.496	10
HAT	LYZ	Lysozyme	0.06879739	0.496	10
HAT	TNF	Tumor necrosis factor	0.02504945	0.48062016	7
HAT	ABAT	4-aminobutyrate aminotransferase	0.00544716	0.47328244	7
HAT	GPI	Glucose-6-phosphate isomerase	0.00544716	0.47328244	5
HAT	CTSD	Cathepsin D	0.00544716	0.47328244	5
HAT	CTSB	Cathepsin B	0.00544716	0.47328244	5
HAT	UROD	Uroporphyrinogen decarboxylase	5.24E-05	0.46616541	3
HAT	TREH	Trehalase	5.24E-05	0.46616541	3
HAT	SPR	Sepiapterin reductase	5.24E-05	0.46616541	3

Protein protein interaction (PPI) network was constructed in the String database and visualized in Cytoscape 3.7.2. The results are shown in Figure 6. The analysis results showed that CAT, GAPDH, HMOX1, CTH, SHMT2, SHMT1, TNF, MPO, AHCY and GPI, played an essential role in the anti-inflammatory process of AT and HAT.

GO AND KEGG ENRICHMENT ANALYSIS

DAVID database was used to analyze the functional enrichment analysis of the key targets to study the functions of these targets holistically. Forty-nine biological processes (BPs), fifteen molecular functions (MFs) and eleven cellular components (CCs) were enriched from AT and HAT. The top twenty biological processes are shown in Figure 7. These targets were involved in various biological processes, including protein homotetramerization, hydrogen sulfide biosynthetic process, transsulfuration, l-serine metabolic process and protein tetramerization. The results illustrated that the volatile components of AT and HAT play an anti-inflammatory role by regulating these similar biological processes.

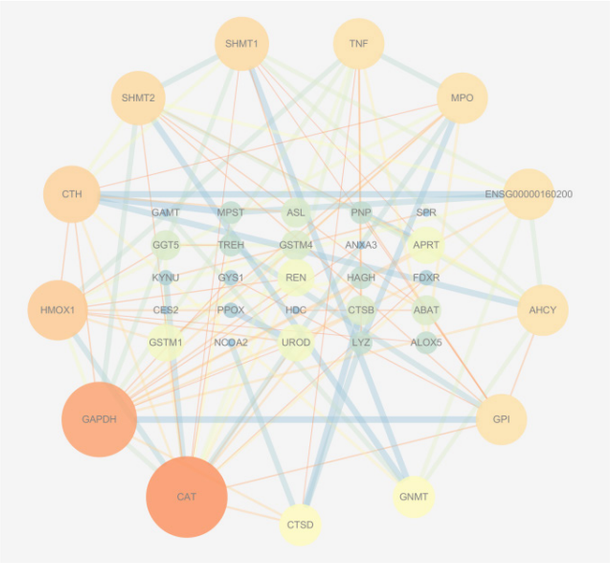

FIGURE 6. PPI network of AT and HAT volatile oil anti-inflammation

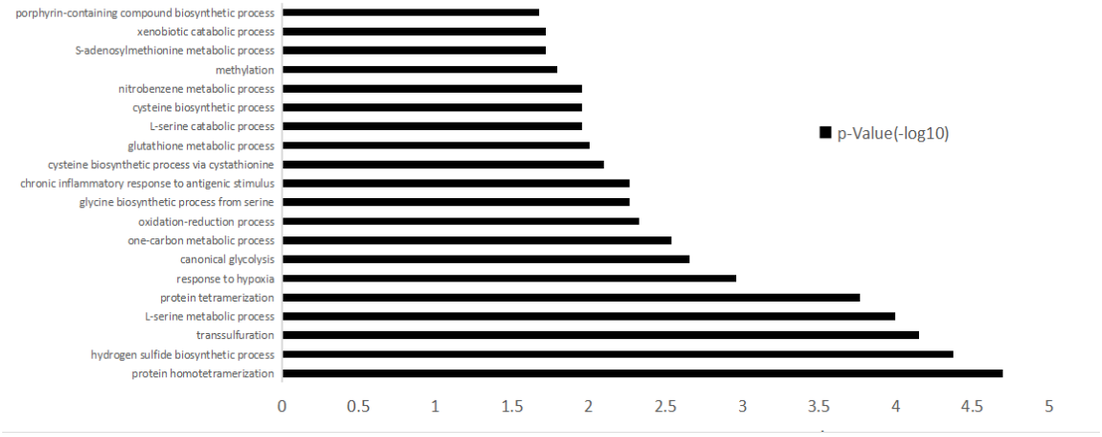

FIGURE 7. Go biological process analysis of AT and HAT volatile oil anti-inflammation

KEGG pathways were mainly associated with glycine, serine and threonine metabolism; biosynthesis of amino acids; biosynthesis of antibiotics; and cyanoamino acid metabolism (Figure 8). Using the KEGG mapper function in the KEGG signalling pathway database, the key target genes and the target proteins associated with inflammation were marked on the most closely related signal pathway, and similar anti-inflammatory targets of AT and HAT were marked in red. The results are shown in Figure 9.

DOCKING RESULTS

The nodes with a high degree value in PPI were considered as the essential proteins. In this study, AT and HAT's top ten key proteins include SHMT1, CAT, GPI, AHCY, HMOX1, CTH, MPO, TNF, SHMT2, and GAPDH, were used for molecular docking with the active ingredients with the highest content in AT and HAT. The results showed the ten proteins with a strong affinity for humulene, γ-muurolene, α-phellandrene, and acetic acid. Therefore, the volatile components of AT and HAT play an essential role in anti-inflammatory action. The docking scores are shown in Figures 10 and 11.

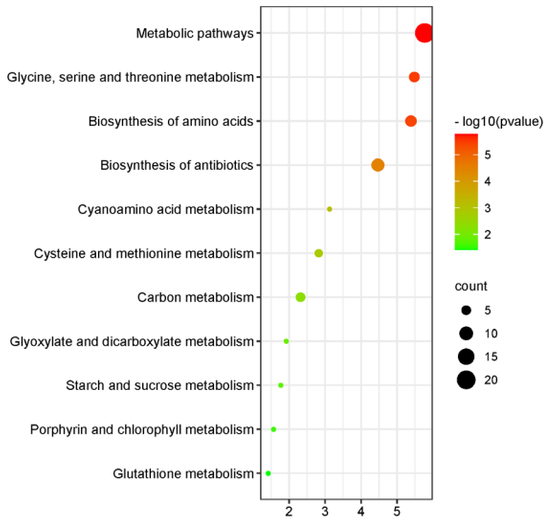

FIGURE 8. KEGG pathways analysis of AT and HAT volatile oil anti-inflammation

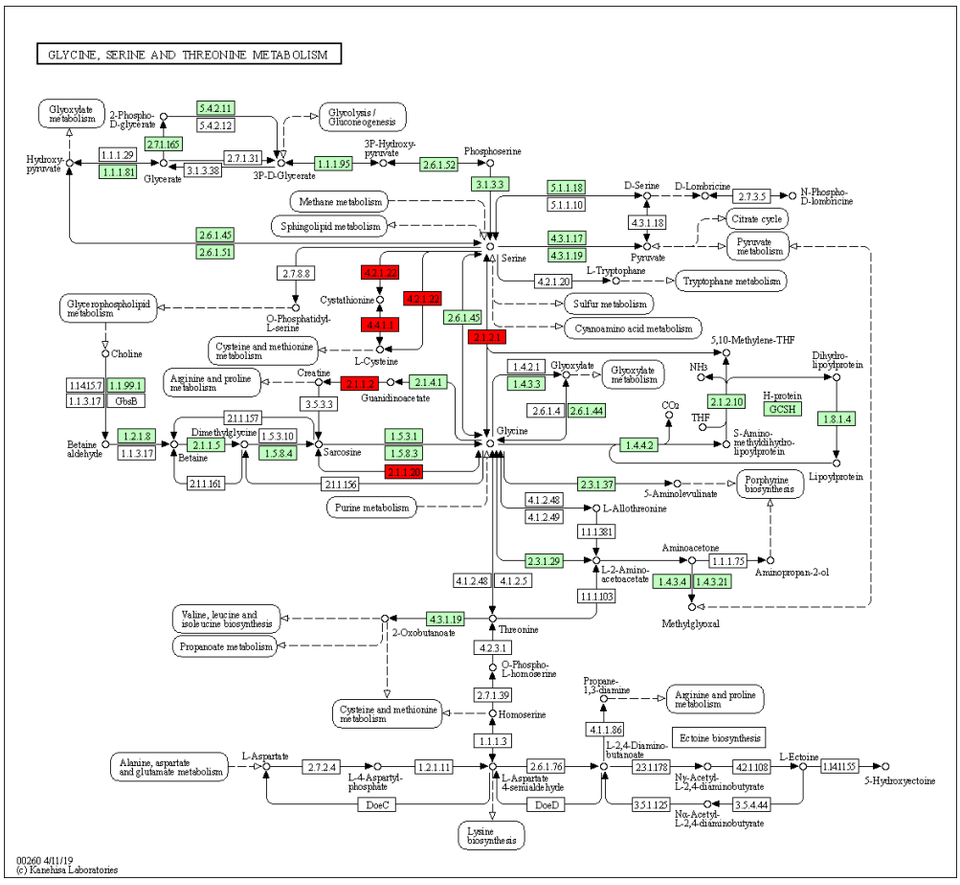

FIGURE 9. Glycine, serine and threonine metabolism annotated signalling pathway diagram

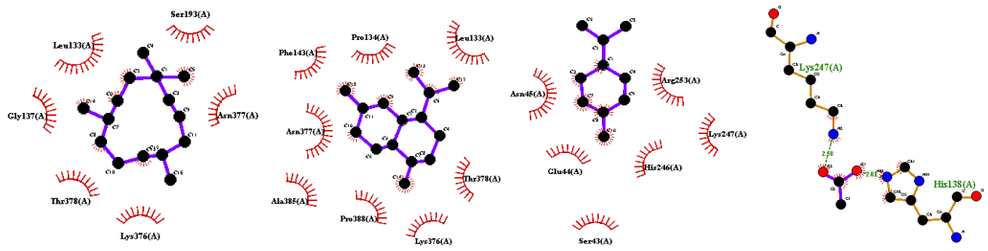

A B C D

SHMT1(PDB ID: 1bj4)

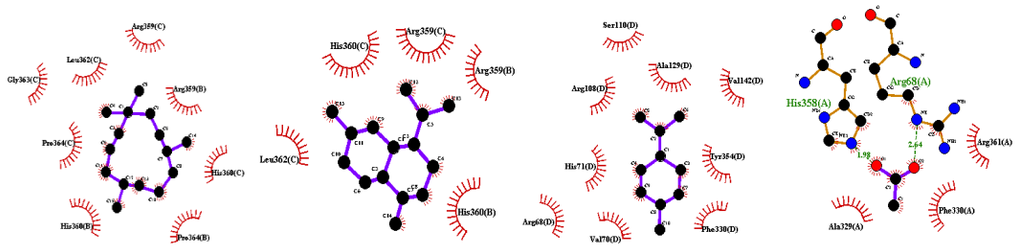

A B C D

CAT(PDB ID: 1dgf)

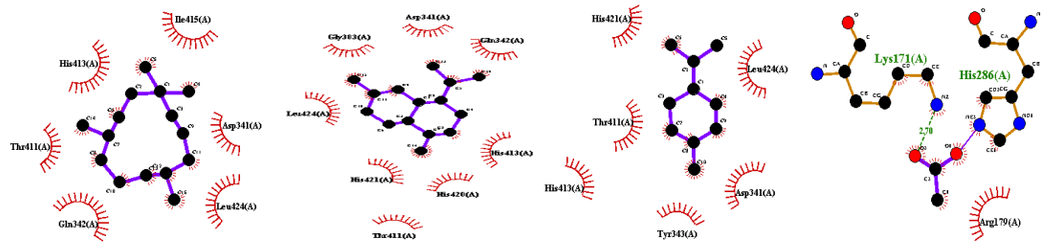

A B C D

GPI(PDB ID: 1iat)

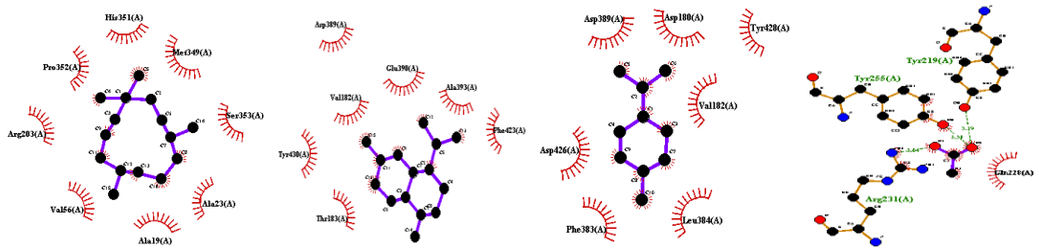

A B C D

AHCY(PDB ID: 1li4)

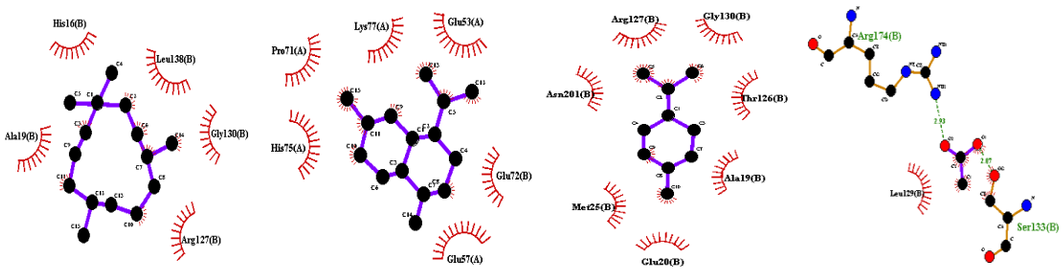

A B C D

HMOX1(PDB ID: 1n45)

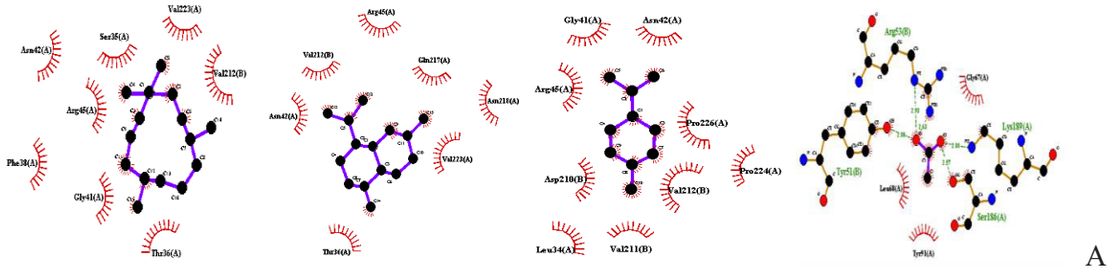

A

B C D

CTH(PDB ID: 3cog)

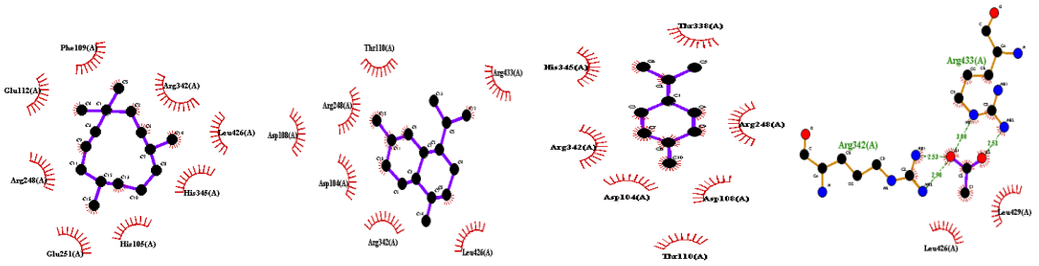

A B C D

MPO(PDB ID: 5mfa)

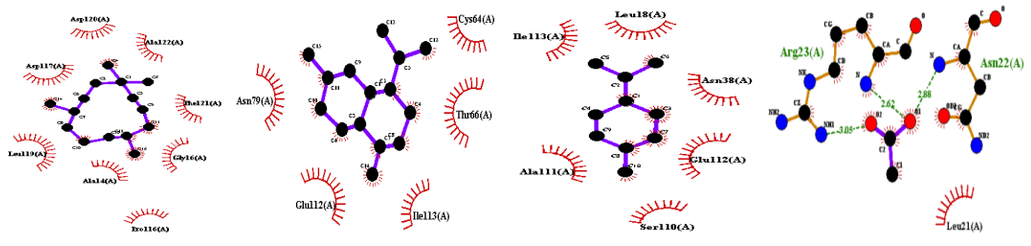

A B C D

TNF(PDB ID: 5uui)

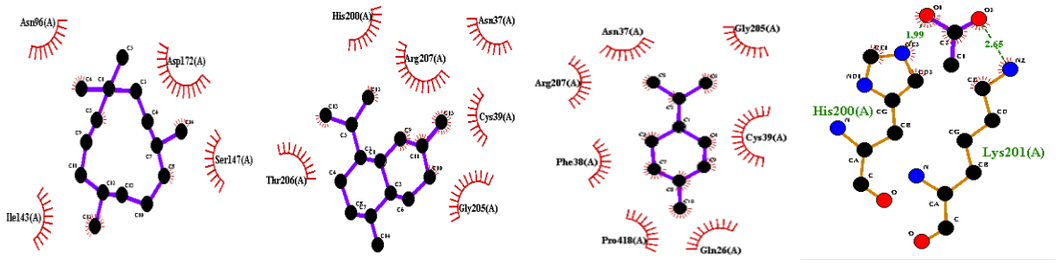

SHMT2(PDB ID: 6dk3)

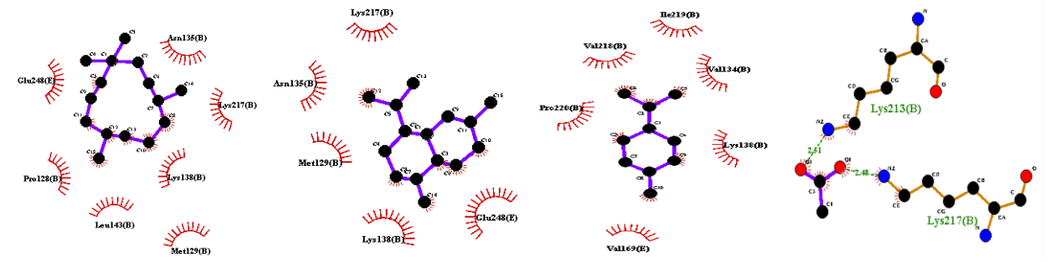

GAPDH(PDB ID: 6ynd)

FIGURE 10. Molecular docking results (A: humulene; B: γ-muurolene; C: α-phellandrene; D: acetic acid)

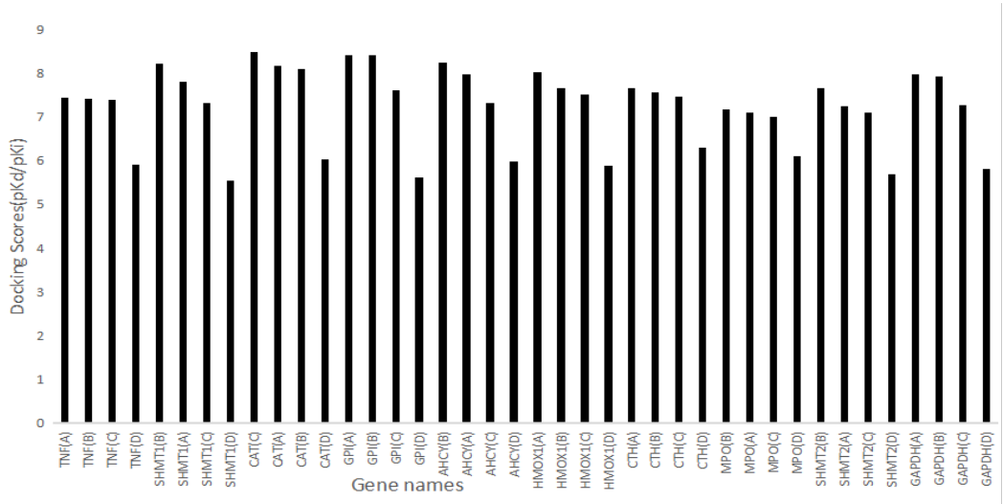

FIGURE 11. Molecular docking scores of AT and HAT (A: humulene; B: γ-muurolene; C: α-phellandrene; D: acetic acid)

THE SIMILARITIES AND DIFFERENCES OF AN ANTI-INFLAMMATORY MECHANISM

The volatile components of AT and HAT predicted by GC-MS and network pharmacology have anti-inflammatory effects. These findings are consistent with those reported in related literatures. The results are shown in Tables 4 and 5.

TABLE 4. similarities of anti-inflammation between AT and HAT

Type	Similarities	Reference
Potential active components	ethanol, acetic acid, benzaldehydem, α-phellandrene, p-cymene, acetophenone, humulene, γ-muurolene, methyl palmitate	The pharmacodynamic experiment showed that p-cymene has an anti-inflammatory effect (Leonardo et al. 2012) Methyl palmitate is a universal macrophage inhibitor, and it has an anti-inflammatory effect (Ebtehal 2011)
Key targets	CTSB, CTSD, GPI, HDC, PNP, CBS, F7, KYNU, TNF, AHCY, CAT, CES2, PFKFB4, LYZ, GYS1, GAPDH, ABAT, HMOX1, FDXR, SHMT2, SHMT1, F13A1, UROD, APRT, GSTM1, ANXA3, CPA1, CTH, GNMT, HAGH, GPHN, GSTM4, HDAC8, GAMT, ALOX5, MMUT, PPOX, MPST, ASL, LCMT2, PYCR2, SPR, GGT5, MPO, REN, TREH , NCOA2	Catalase (CAT) is the most important intracellular enzyme, and it could suppress periodontal inflammation in beagles (Petelin et al. 2000) One of the bacterial surface Plg receptors is the multifunctional glycolytic enzyme glyceraldehyde-3-phosphate dehydrogenase (GAPDH). Recent research suggested that when upon inflammation, macrophages recruit GAPDH onto their surface to carry out a similar task of capturing Plg to digest extracellular matrix to aid rapid phagocyte migration and combat the invading pathogens (Chauhan et al. 2017)
Pathways	Metabolic pathways; Glycine, serine and threonine metabolism; Biosynthesis of amino acids; Biosynthesis of antibiotics; Cyanoamino acid metabolism; Cysteine and methionine metabolism; Carbon metabolism; Glyoxylate and dicarboxylate metabolism; Starch and sucrose metabolism; Porphyrin and chlorophyll metabolism; Glutathione metabolism	According to the reports, the increased proliferation and rapid activation of immune cells during inflammation require a switch in cell metabolism from a resting regulatory state to a highly metabolically active state to maintain energy homeostasis. This metabolic shift occurs in many inflammatory conditions such as colitis, diabetes, psoriasis, obesity and rheumatoid arthritis (Ping et al. 2015; Trudy et al. 2017) Glycine, serine and threonine metabolism were the main biomarkers of the antiarthritic mechanism of moxibustion (Pang et al. 2021)

TABLE 5. Differences of anti-inflammation between AT and HAT

Type	Differences	Reference
potential active components of HAT	methyleugenol, β-elemene , furfural	Methyleugenol (ME) is a natural compound with antiallergic, and anti-inflammatory effects. ME markedly reduced the production of the proinflammatory lipid mediators prostaglandin E2, prostaglandin D2, leukotriene B4, and leukotriene C4. Furthermore, it could inhibit allergic response by suppressing the activation of Syk, ERK1/2, p38, JNK, cPLA2, and 5-LO (Feng et al. 2015) β-elemene treatment modulated immune balance in the periphery and the inflamed optic nerve by promoting less downregulation in Treg cells, inhibiting Th17 and Th1 polarization (Zhang et al. 2010). Therefore, β-elemene induces substantial protection in experimental autoimmune encephalomyelitis optic nerve. Meanwhile, β-elemene is a natural antitumor plant drug (Bai et al. 2021)
potential active targets of HAT	EIF6, PKIA	Eukaryotic translation initiation factor 6 (EIF6) could inhibit the expression of inflammatory mediators of M2 macrophages and then inhibit the production of vascular endothelial growth factors from preventing the excessive proliferation of blood vessels and granulation tissue (Wen et al. 2015). It suggests that HAT has the potential to prevent the excessive proliferation of blood vessels and granulation tissue Hepatocellular carcinoma, a slow multistep process, eventually starts from long-term inflammation to fibrosis and leads to malignancy. Protein kinase A is one of them, significantly contributes to liver tumorigenesis by stimulating cyclic AMP. Its inhibitor, cAMP-dependent protein kinase inhibitor alpha (PKIA), plays a significant role in inhibiting hepatic tumerogenesis (Riggle et al. 2016), so PKIA can improve the tumour by preventing inflammation. It suggested that HAT had a potential therapeutic effect on tumours The results showed that different anti-inflammatory active components were produced in different processing processes, and then different anti-inflammatory targets were produced

CONCLUSIONS

In summary, the obtained results by GC/MS indicated significant differences in volatile compositions and percentages between AT and HAT. After honey processing, HAT reduced sixteen volatile components

and increased twelve volatile components. Moreover, the anti-inflammatory mechanism of volatile components of Hebei AT before and after honey-fried had prominent similarities and smaller differences. HAT can play an anti-inflammatory role through its unique active ingredients and key targets, indicating that HAT has its characteristics in clinical anti-inflammatory. Nevertheless, their active anti-inflammatory components and percentage contents were different, and HAT was higher than AT. Therefore, the anti-inflammatory effect of volatile components of HAT may be better than that of AT. HAT has a better effect than AT in eliminating phlegm (Wu et al. 2006). It is possible that the volatile oil components of AT changed in the process of honey-fried, which enhanced the anti-inflammatory effect and then enhanced the expectorant effect of HAT. This study laid a theoretical foundation for the anti-inflammatory mechanism of AT and HAT and provided a theoretical basis for whether AT and HAT should be treated differently in future research.

ACKNOWLEDGEMENTS

This work was supported by the Guizhou Domestic First-Class Construction Project ((Chinese Materia Medica) (GNYL (2017) 008)).

REFERENCES

Bai, Z.Q., Yao, C.S., Zhu, J.L. & Xie, Y.Y. 2021. Anti-tumor drug discovery based on natural product β-elemene: Anti-tumor mechanisms and structural modification. *Molecules* 26(6): 1499.

Bonjardim, L.R., Cunha, E.S., Guimarães, A.G., Santana, M.F., Oliveira, M.G., Serafini, M.R., Araújo, A.A., Antoniolli, Â.R., Cavalcanti, S.C., Santos, M.R. & Quintans-Júnior, L.J. 2012. Evaluation of the anti-inflammatory and antinociceptive properties of p-cymene in mice. *Zeitschrift für Naturforschung C* 67(1-2): 15-21.

Chauhan, A.S., Kumar, M., Chaudhary, S., Patidar, A., Dhiman, A., Sheokand, N., Malhotra, H., Raje, C.I. & Raje, M. 2017. Moonlighting glycolytic protein glyceraldehyde-3-phosphate dehydrogenase (GAPDH): An evolutionarily conserved plasminogen receptor on mammalian cells. *The Federation of American Societies for Experimental Biology Journal* 31(6): 2638-2648.

Dutta, P., Sahu, R.K., Dey, T., Lahkar, M.D., Manna, P. & Kalita, J. 2019. Beneficial role of insect-derived bioactive components against inflammation and its associated complications (colitis and arthritis) and cancer. *Chemico-Biological Interactions* 313(2019): 108824.

Ebtehal, E. 2011. Anti-inflammatory and antifibrotic effects of methyl palmitate. *Toxicology and Applied Pharmacology* 254(3): 238-244.

Fang, H.Y., Shan, G.W., Qin, G.F., Zhen, L., Li, M.H. & Hao, L.J. 2012. Advances on chemical components and pharmacological actions of *Aster tataricus*. *Medical Research and Education* 29(5): 73-77.

Feng, T., Feilong, C., Xiao, L., Huang, Y., Zheng, X., Tang, Q. & Tan, X. 2015. Inhibitory effect of methyleugenol on IgE-mediated allergic inflammation in RBL-2H3 cells. *Mediators of Inflammation* 2015: 463530.

Fink, T., Wolf, A., Maurer, F., Albrecht, F.W., Nathalie, H., Beate, W., Hauschild, A.C., Bertram, B., Baumbach, J.I. & Thomas, V. 2015. Volatile organic compounds during inflammation and sepsis in rats: A potential breath test using ion-mobility spectrometry. *Anesthesiol* 122(1): 117-126.

Gong, Q.F. 2016. *Traditional Chinese Medicine Processing: Chapter XII.* Beijing: China Press of Traditional Chinese Medicine.

Guo, C., Kang, X.D., Cao, F., Yang, J. & Fu, X. 2021. Network pharmacology and molecular docking on the molecular mechanism of Luo-Hua-Zi-Zhu (LHZZ) granule in the prevention and treatment of bowel precancerous lesions. *Frontiers in Pharmacology* 12: 1-14.

Huang, X., Gao, Y., Xu, F., Fan, D. & Wu, H. 2020. Molecular mechanism underlying the anti-inflammatory effects of volatile components of *Ligularia fischeri* (Ledeb) Turcz based on network pharmacology. *BMC Complementary Medicine and Therapies* 20(1): 1-13.

Labib, R.M., Youssef, F.S., Ashour, M.L., Abdel-Daim, M.M. & Ross, S.A. 2017. Chemical composition of *Pinus roxburghii* bark volatile oil and validation of its anti-inflammatory activity using molecular modelling and bleomycin-induced inflammation in albino mice. *Molecules* 22(9): 1384.

Li, C., Huang, F., Dou, C.G., Zhang, M. & Ma, S.P. 2009. Effect of compatibility of *Aster tataricus* and Flos Farfarae on anti-inflammation. *Chinese Journal of Clinical Pharmacology and Therapeutics* 14(2): 155-159.

Li, M.Q., Luo, L., Shang, N.N., Meng, B.H. & Huang, H.Z. 2020. Contradictions and countermeasures from cultural inheritance to industrial modernization. *Chinese Traditional Patent Medicine* 42(11): 2999-3003.

Li, P., Wang, J., Wang, C., Cheng, L. & Zhao, B. 2021. Therapeutic effects and mechanisms study of Hanchuan Zupa Granule in a guinea pig model of cough variant asthma. *Journal of Ethnopharmacology* 269(6): 113719.

Li, S.M., Zeng, B.Y., Ye, Q., Ao, H. & Li, H.X. 2015. Correlation analysis between GC-MS fingerprint of essential oil of amomi fructus and antiinflammatory activity. *Chinese Journal of Experimental Traditional Medical Formulae* 21(9): 133-136.

Lin, Z.X. 2011. Benzylamine and methylamine, substrates of semicarbazide-sensitive amine oxidase, attenuate inflammatory response induced by lipopolysaccharide. Thesis. Shantou University (Unpublished).

Lin, Y.M., Badrealam, K.F., Kuo, W.W., Lai, P.F., Chen, W.S., Day, C.H., Ho, T.J., Viswanadha, V.P., Shibu, M.A. & Huang, C.Y. 2020. Nerolidol improves cardiac function in spontaneously hypertensive rats by inhibiting cardiac inflammation and remodelling associated TLR4/ NF-κB signalling cascade. *Food and Chemical Toxicology* 147(2021): 111837.

McGarry, T., Biniecka, M., Gao, W., Cluxton, D., Canavan, M., Wade, S., Wade, S., Gallagher, L., Orr, C., Veale, D.J. & Fearon, U. 2017. Resolution of TLR2-induced inflammation through manipulation of metabolic pathways in Rheumatoid Arthritis. *Scientific Reports* 7: 43165.

National Pharmacopoeia Commission. 2020. *The Pharmacopoeia of the People's Republic of China: Part I.* Beijing: China Medical Science and Technology Press.

Ninomiya, K., Hayama, K., Ishijima, S.A., Maruyama, N., Irie, H., Kurihara, J. & Abe, S. 2013. Suppression of inflammatory reactions by terpinen-4-ol, a main constituent of tea tree oil, in a murine model of oral candidiasis and its suppressive activity to cytokine production of macrophages *in vitro*. *Biological and Pharmaceutical Bulletin* 36(5): 838-844.

Pang, X.T., Zhang, Y.Y., Leng, Y.F., Yao, Y., Zhang, R., Wang, D.W., Xu, X. & Sun, Z.L. 2021. Metabolomics study of biochemical changes in the serum and articular synovium tissue of moxibustion in rats with collagen-induced arthritis. *World Journal of Acupuncture-Moxibustion* 31(1): 30-43.

Petelin, M., Pavlica, Z., Ivanuša, T., Šentjurc, M. & Skalerič, U. 2000. Local delivery of liposome-encapsulated superoxide dismutase and catalase suppress periodontal inflammation in beagles. *Journal of Clinical Periodontology* 27(12): 918-925.

Ping, J., Hao, L. & Xiao, L. 2015. Diabetes mellitus risk factors in rheumatoid arthritis: A systematic review and meta-analysis. *Clinical and Experimental Rheumatology* 33(1): 115-121.

Queiroz, J.C.C., Antoniolli, Â.R., Quintans-Júnior, L.J., Brito, R.G., Barreto, R.S., Costa, E.V., da Silva, T.B., Prata, A.P.N., de Lucca, W., Almeida, J.R. & Lima, J.T. 2014. Evaluation of the anti-inflammatory and antinociceptive effects of the essential oil from leaves of *Xylopia laevigata* in experimental models. *The Scientific World Journal* 2014: 816450.

Riggle, K.M., Riehle, K.J., Kenerson, H.L., Turnham, R., Homma, M.K., Kazami, M., Samelson, B., Bauer, R., McKnight, G.S. & Scott, J.D. 2016. Enhanced cAMP-stimulated protein kinase A activity in human fibrolamellar hepatocellular carcinoma. *Pediatric Research* 80: 110-118.

Saeed, N.M., Ebtehal, E.D., Hanaa, M.A., Algandaby, M.M., Fahad, A.A. & Ashraf, B.A. 2012. Anti-inflammatory activity of methyl palmitate and ethyl palmitate in different experimental rat models. *Toxicology and Applied Pharmacology* 264(1): 84-93.

Santos, K.B., Guedes, I.A., Karl, A.L. & Dardenne, L.E. 2020. Highly flexible ligand docking: Benchmarking of the DockThor program on the LEADS-PEP protein–peptide data set. *Journal of Chemical Information and Modeling* 60(2): 667-683.

Sakhaee, M.H., Sayyadi, S.A.H., Sakhaee, N., Sadeghnia, H.R., Hosseinzadeh, H., Nourbakhsh, F. & Forouzanfar, F. 2020. Cedrol protects against chronic constriction injury-induced neuropathic pain through inhibiting oxidative stress and inflammation. *Metabolic Brain Disease* 35(7): 1119-1126.

Sousa, C., Leitão, A.J., Neves, B.M., Judas, F., Cavaleiro, C. & Mendes, A.F. 2020. Standardized comparison of limonene-derived monoterpenes identifies structural determinants of anti-inflammatory activity. *Scientific Reports* 10(1): 7199.

Su, G.Y. & Liu, Y. 2011. Production process of *Aster tataricus* and honey-fried *Aster tataricus. Capital Medicine* 18(3): 49.

Wen, S., Hu, X.H., Zhang, X.R. & Huang, Y. 2015. Effects of eIF6 on the expression of pro-inflammatory mediators derived from M2 macrophages. *Medical Journal of Chinese People's Liberation Army* 40(2): 104-109.

Wu, C., Chen, Z.J., Hu, Y.J., Xiu, Y.F. & Cheng, X.M. 2006. Experimental study on phlegm-resolving action of different prepared products of radix Asteris. *Journal of Shanghai University of Traditional Chinese Medicine* 20(3): 55-57.

Yang, Q., Luo, J., Lv, H., Wen, T. & Zeng, N. 2019. Pulegone inhibits inflammation via suppression of NLRP3 inflammasome and reducing cytokine production in mice. *Immunopharmacology and Immunotoxicology* 41(3): 1-8.

Zhang, H.P., Li, D.X. & Zhou, Y. 2017. Anti-inflammatory, antitussive, expectorant and analgesic effects of volatile oil from Uighur medicine *Hyssopus officinalis*. *China Pharmacist* 20(2): 221-224.

Zhang, R.W., Tian, A., Shi, X.G. & Yu, H.M. 2010. Downregulation of IL-17 and IFN-γ in the optic nerve by β-elemene in experimental autoimmune encephalomyelitis. *International Immunopharmacology* 10(7): 738-743.

*Corresponding author; email: whm0425@126.com